ISSN 2529-9824

Artículo de Investigación

Fostering technological progress in space exploration to drive Sustainable Development Goals

Potenciar los ODS a través del avance tecnológico en la exploración espacial

Raquel Caro-Carretero[1]: Universidad Pontificia Comillas de Madrid. Cátedra de Catástrofes Fundación AON España. España.

Fecha de Recepción: 23/05/ 2024

Fecha de Aceptación: 28/06/2024

Fecha de Publicación: 03/07/2024

Cómo citar el artículo (APA 7ª):

Caro-Carretero, R. (2025). Fostering Technological Progress in Space Exploration to Drive Sustainable Development Goals [Potenciar los ODS a través del avance tecnológico en la exploración espacial]. *European Public & Social Innovation Review*, 10, 1.-19. https://doi.org/10.31637/epsir-2025-323

Abstract:

Introduction: Exploration of space and gathering data on its atmospheric conditions could drive the development of advanced space technologies, such as atmospheric sensors and remote monitoring systems. Then, scientific research in seemingly distant areas, such as astrophysics and space exploration, can contribute to the achievement of the SDGs by promoting innovation and sustainable technological development. **Methodology**: We present an automated four-step detection algorithm for identification of photoelectron peaks based on a short-term-average/long-term-average phase picker taken along a characteristic function. Additional analysis is applied to the longer signal window after the declared detection to characterize photoelectron peaks and discard noise disturbances. **Results:** The modular design of the algorithm enables the substitution of alternative strategies in any of the four steps and the rapid implementation on new datasets. **Discussion:** The utility of the algorithm is illustrated through an overview example based on data from all available Titan flybys. The knowledge about photoelectron peaks in Titan's atmosphere could offer insights that could be valuable for addressing climate change on Earth. **Conclusions**: Understanding planetary plasma environments, including their interaction with the solar wind and other space weather phenomena, can indirectly contribute to our understanding of Earth's climate system.

Keywords: SDG 9; the Cassini mission's Electron Spectrometer (CAPS-ELS); photoelectron

[1] **Autor Correspondiente:** Raquel Caro-Carretero. Universidad Pontificia Comillas de Madrid

peaks; Titan's atmosphere; innovation; sustainable technological development; automated four-step detection algorithm; Earth's climate system.

Resumen:
Introducción: La exploración del espacio y la recopilación de datos sobre sus condiciones atmosféricas pueden impulsar el desarrollo de tecnologías espaciales avanzadas, como sensores atmosféricos y sistemas de monitoreo remoto. La investigación científica en áreas aparentemente distantes, como la astrofísica y la exploración espacial, puede contribuir al logro de los ODS al promover la innovación y el desarrollo tecnológico sostenible. **Metodología:** Presentamos un algoritmo automatizado de detección en cuatro pasos para la identificación de picos de fotoelectrones utilizando una técnica utilizada en sismología que se basa en la relación entre dos promedios móviles de la señal. Para caracterizar los picos y descartar perturbaciones de ruido se aplica un análisis adicional después de la detección declarada. **Resultados:** El diseño modular del algoritmo permite la sustitución de estrategias alternativas en cualquiera de los cuatro pasos y la implementación rápida en nuevos conjuntos de datos. **Discusiones:** La utilidad del algoritmo se ilustra a través de un ejemplo general basado en datos de todos los sobrevuelos disponibles de Titán. **Conclusiones:** Comprender los entornos de plasma planetario, incluida su interacción con el viento solar y otros fenómenos meteorológicos espaciales, puede contribuir indirectamente a nuestra comprensión del sistema climático de la Tierra.

Palabras clave: ODS 9; Espectrómetro de Electrones (CAPS-ELS) de la misión Cassini; fotoelectrones; atmósfera de Titán; innovación; desarrollo tecnológico sostenible; algoritmo automatizado de detección en cuatro pasos; sistema climático de la Tierra.

1. Introduction

Progress in physics, as in the other sciences, arises from a close interplay of experiment and theory. In fact, in the history of the physical sciences, the development of theory and application of good principles of measurement have gone hand in hand: each has informed the other. What is more, in many ways, the physical sciences are at the forefront of using digital tools and statistical methods for data analysis. The fields and disciplines that make up the physical sciences are by no means uniform, and scientists find, work and share information and data in richly varied ways, though. In this regard, studies emphasize the value of examining Titan's atmospheric and environmental processes to draw parallels with Earth's own climate system, potentially offering new methods and models to address climate change challenges. Cloud formation and precipitation of methane can inform us about non-water-based climatic cycles on Earth and potential climate mitigation strategies (Mitchell & Lora, 2016). These interactions could shed light on the prebiotic chemistry relevant to early Earth conditions (Hörst, 2017). Gu et al. (2019) have highlighted the dynamics of chemical species like nitrogen and carbon in Titan's atmosphere, which can shed light on atmospheric escape mechanisms. These studies are crucial for understanding the long-term climate evolution on terrestrial planets. Observations from Cassini have revealed how temperatures in Titan's lower stratosphere evolve with the seasons, showing significant seasonal changes, particularly at the poles. Understanding these thermal responses to seasonal and meridional insolation variations can enhance our knowledge of similar atmospheric behaviors on Earth (Sylvestre et al., 2020). Crósta et al. (2021) explores how the formation of impact craters on Titan, such as the Menrva crater, could influence the habitability of planetary bodies by enabling the exchange of materials between the surface and subsurface. This has implications for understanding the conditions favorable for life and prebiotic chemistry on other celestial bodies. Furthermore, the global climate models of Titan can help us understand the atmospheric circulation and seasonal effects, which are applicable to studying Earth's past and

future climate scenarios. These models are crucial in understanding how atmospheric processes can be influenced by various planetary characteristics [Friedson et al., 2009]. A mathematical climate model of Titan's atmosphere, which considers the atmospheric mass motion and energy circulation processes, provides insights that can be analogous to studying similar processes on Earth (Mulholland & Wilde, 2020). This model explores how solar energy is retained in the atmosphere, helping to understand fundamental meteorological processes like the Hadley cell on terrestrial planets.

Ultimately, research on Titan's atmosphere and its implications for understanding climate phenomena can offer valuable insights into Earth's own climate systems. Understanding planetary plasma environments, including their interaction with the solar wind and other space weather phenomena, can indirectly contribute to our understanding of Earth's climate system. In particular, the knowledge about photoelectron peaks in Titan's atmosphere could offer insights that could be valuable for addressing climate change on Earth. Discrete peaks near 24,1 eV are observed in Titan's ionosphere, generated by ionization of N2 due to solar radiation. These photoelectrons are predominantly found in the dayside ionosphere and can be used as tracers of magnetic field lines, which might help in understanding the plasma environments of other planetary bodies (Wellbrock et al., 2012). Studying the ionization processes and resultant photoelectron emissions in Titan's atmosphere might help in modeling complex atmospheric chemistry and interactions in Earth's upper atmosphere, especially those involving nitrogen compounds. Such studies could potentially offer new perspectives in managing solar radiation or developing strategies related to atmospheric chemistry management for climate mitigation. The methodologies used in detecting and analyzing these photoelectron peaks on Titan could enhance techniques for studying similar phenomena in Earth's atmosphere. This could be crucial for better understanding the dynamics of Earth's ionosphere and its implications on climate and environmental science. Broadly, studies of Titan's atmosphere can enrich our general understanding of atmospheric processes, potentially offering analogs or contrasts to Earth's climatic and atmospheric systems which could inform climate change mitigation strategies. The exploration of Titan's photoelectron peaks thus not only could enrich planetary science but also holds a mirror up to Earth's own atmospheric studies, offering tools and insights that could be beneficial in our quest to assist in predicting extreme weather events and assessing adaptation strategies. Space weather events, driven by variations in the solar wind and magnetic activity, can have indirect effects on Earth's climate. For example, geomagnetic storms can induce changes in atmospheric circulation and temperature, affecting weather patterns and climate variability. Photoelectron measurements provide insights into the dynamics of the upper atmosphere, including ionization processes and the formation of plasma layers. Changes in the upper atmosphere can influence climate by altering the balance of greenhouse gases, ozone distribution, and atmospheric chemistry.

Here we introduce an algorithm that automatically detects peaks in electron data measured by the Cassini-Huygens mission in order to improve our understanding of the plasma environments around the moons and planets in the solar system. The Cassini-Huygens missions is a joint NASA (2023), ESA (European Space Agency) and ASI (Italian Space Agency) mission and was in orbit around the planet Saturn from 2004 to 2017. It studied the planet and its rings, moons, and neutral and plasma environment. In this study we focus on applying our algorithm to study the plasma environment of Saturn’s largest moon, Titan; however, the algorithm can be applied to a variety of datasets. Titan is unique in the solar system because it is the only moon which has an extended atmosphere, denser than even most known planets (Brown et al., 2010; Hörst, 2017). This atmosphere is nitrogen based with large concentrations of organic molecules, resulting in highly complex organic chemistry taking place at a large range of altitudes, including the topside ionosphere which is >1.000km from the surface. The

Cassini orbiter regularly passed through this region and took measurements using its suite of in-situ instruments. Titan's orbit is located at 20 Saturn radii (1 RS = 60.268 km), placing it (under standard solar wind dynamic pressure) in the outer part of a region called Saturn's magnetosphere. This region and its dynamics are dominated by Saturn's rotation and planetary magnetic field (Neubauer et al., 1984); it shields the planet and its moons and rings from the solar wind. Titan itself does not have an intrinsic magnetic field, however Titan's atmosphere interacts with the plasma in Saturn's outer magnetosphere and forms an induced magnetosphere (Cravens et al., 2009; Wellbrock et al., 2012). This interaction is similar to the solar wind interaction with globally unmagnetised objects such as Venus, Mars and comets. One way to improve our understanding of this type of interaction is to try to find particles that can trace magnetic field lines from the low upstream ionosphere to the distant tail. Photoelectrons are mobile along magnetic field lines and so when they are observed distant from their source, they can be used to constrain the field line morphology (Wellbrock et al., 2012). However, electrons can be produced from a variety of different reactions and it is therefore not possible to determine where particular electrons may have come from, unless the distinct energy signature of photoelectrons produced by the ionization of N2 by the solar He-II line identifies when a field line sampled at the spacecraft location intersects Titan's day-side ionosphere. Such a specific characteristic is present in some photoelectrons and it is these characteristic photoelectrons that our algorithm aims to find in the spacecraft data.

The energy of the photoelectron depends on the energy difference between the incoming photon and the ionization potential and the initial and final excitation states of target species. Therefore, a range of photoelectron energies can generally be observed. However, there is a larger number of photoelectrons with a specific energy due to the ionization of neutrals by the particularly strong He-II 30.4nm (40,79 eV) solar emission line. As a result, photoelectron peaks can be observed in planetary atmospheres' electron energy spectra, and it is the characteristic energy of this peak that makes these photoelectrons particular useful. At Titan, this characteristic energy is 24,1 eV due to the ionization of nitrogen molecules by the He-II 30.4nm line.

Photoelectrons are found on the dayside of Titan's upper neutral atmosphere/ionosphere and can be observed in electron energy spectra from the Electron Spectrometer (ELS) part of the Cassini Plasma Spectrometer (CAPS) because this is where neutral nitrogen molecules are present, and solar radiation can reach these and ionize them (Young et al., 2004). We therefore expect the production sites of the 24,1 eV electrons to be in this environment (Haider, 1986; Gan et al., 1992). However, some photoelectrons are also observed at other locations where local production is unlikely (e.g. Wellbrock et al., 2012); at higher altitudes, due to lack of sufficient neutral molecules, and on the nightside, due to lack of solar radiation. They can travel to these observation sites via magnetic field lines. When we detect such photoelectron peaks at high altitudes and on the nightside, we know due to their characteristic peak energy that they were produced remotely and traveled to the observation site via magnetic field lines. This is what makes these photoelectron peak observations particularly useful for tracing magnetic field lines and hence improving our understanding of the plasma environment. However, the photoelectron exobase of Titan, above which the photoelectron collisions with ambient neutral particles become negligible, locates at the altitude of ~1.505 km (Cao et al., 2020).

In addition, a steep decrease in the intensity of the solar spectrum for wavelengths ~20 nm and below results in a reduction of the photoelectrons observed at and above ~60 eV (e.g. Nagy et al., 1977; Fox and Dalgarno, 1979). These signatures are present in the electron spectra previously predicted for Titan (Gan et al., 1992; Cravens et al., 2009) and described by Galand et al. (2010) using Cassini data. Observing this decrease in the data indicates an additional characteristic of primary photoelectron production.

Photoelectron peaks due to the He(II) emission lines can also be observed in many other places in the Solar System. The peak energy varies slightly because the neutral species are different, and therefore the ionization potentials are, too. At Earth, photoelectrons have been studied in some detail e.g. by Coates et al. (1985). Photoelectrons have also been observed by Cassini in the Saturn system in the ring exosphere (Coates et al., 2005), throughout the neutral-rich inner magnetosphere (Schippers et al., 2008, 2009) and at Enceladus (Coates et al., 2007, 2010, 2013; Ozak et al., 2012, Taylor et al., 2018). Several spacecraft have made in-situ measurements of photoelectron peaks in the induced magnetospheres of Venus (e.g. Tsang et al., 2015 and references therein) and Mars (e.g. Frahm et al., 2006, Coates et al., 2011 and references therein). Studying these has helped improve our understanding of the interaction between the solar wind and these planetary atmospheres, and the resulting magnetic topology.

Locating photoelectron peaks reliably depends strongly upon the precision of peak determination, which can be performed from both observational and theoretical points of views. Nevertheless, with large data sets, manual inspection becomes time consuming. Here we present such a methodology for characterizing photoelectron peaks which can significantly improve finding them in planetary environments accurately and consistently.

1.1. Instrumentation

The CAPS-ELS is a hemispherical top-hat electrostatic analyzer that measures the flux of electrons as a function of energy per charge and direction of arrival (a full description is given by Young et al., 2004, and Linder et al., 1998). The data consists of 63-level energy spectra obtained every 2s with an energy range of 0.6–28.000 eV/q and an energy resolution of 16,7% (dE/E).

CAPS was operational from the beginning of the mission to June 2011 and then from March to June 2012. There are 62 Titan flybys for which CAPS data are available (28 flybys at high altitude (>1.000Km) and 34 flybys at low altitude (<1.000Km). The trajectories of these flybys vary which allows us to investigate different aspects of Titan's local environment.

2. Material and methods

Automatic picking procedures (APP) are needed to handle the bigger datasets and they must be precise, reliable and capable of adapting to different site and/or instrument characteristics. Unlike manual picking, APP save time and should be more consistent since manual peaks can differ between experts. Reliable photoelectron location is limited by the extent to which reliable information can be recovered from these records. Here we introduce an algorithm that automatically detects peaks in electron data.

2.1. Automatic pickers

One of the most commonly used event detection algorithms is the STA/LTA detector (the short term-average/long term average phase picker) based on lower order statistics and proposed by Allen (1982), introducing the concept of the characteristic function (CF, hereafter),

resulting from a nonlinear transformation by which the 'character' of the seismic trace is specified. This algorithm is rapid, simple, robust and easily adaptable and remains useful for identifying events in continuous databases (Baillard et al., 2014) and designed to enhance changes in both amplitude and frequency. Allen's CF is based on the ratio of the two averages calculated on sliding windows over the trace. This STA/LTA approach (termed in seismology literature as a "phase picker detection technique") has been used in Martian studies (Murphy et al., 2002; Ringrose et al., 2007; Aguirre et al., 2017; Xiong et al., 2018). The phase picker detection technique has been demonstrated to give results at terrestrial locations comparable with (much more laborious) manual searches (Jackson & Lorenz, 2015; Lorenz & Lanagan, 2014). The STA/LTA algorithm has also been used to identify and characterize Jupiter's Northern and Southern auroral lightcurves for 24 May (Chandra and XMM-Newton) and 1 June (Chandra) 2016 (Dunn et al., 2017).

2.2. Application of statistical functions for determination of the CF

The event detection algorithm used in this work transforms raw data (x(j) as differential energy flux-DEF-value at a given time and at a specific j-level energy spectrum every 2s) with a CF which could be defined as an 'envelope' of the signal. The signal is characterized by a specific CF, which is used as input information for proposed picker. Such extent that the performance of the picker depends on CF strongly. By and large, the peak detection can be indicated by a change in the frequency, or amplitude, (or both in the time series). CF should enhance the change. Naturally, the CFs based on amplitude of signal (in our case) are not sensitive to periodic changes of signal, and are only sensitive to changes in amplitude.

There are relations between the behavior of the CF of a distribution and properties of the distribution, such as the existence of central statistic moments (lower and higher order statistics). First, in the picking algorithm we introduce here, a CF of a local event is determined as the ratio STA/LTA. The STA measures the instant amplitude of the signal and the LTA contains information about the current average noise amplitude. The peak detection is defined in an energy channel in which the STA/LTA function reaches a user predefined threshold level (STA/ LTA trigger threshold level). The STA/LTA algorithm processes the filtered signal in two moving energy channel windows. Then the CF of a local event is calculated from higher order statistics.

A change in amplitude is recognized by all CFs. However, the CF based on higher order statistics show the most distint pick onset and a simple shape, making it best suitable for picking algorithms. In this way, the photoelectron peak is recognized by each CF, but the CFs calculated from higher order statistics exhibit steeper gradients, which make these CFs very useful for picking techniques.

A fundamental task in many statistical analyses is to characterize the location and variability of a data set (lower order statistics). A further characterization of the data includes higher order statistics such as skewness and kurtosis. Skewness (S, hereafter) is defined in terms of the third central moment. It is a statistical value characterizing the shape of a given distribution. It becomes zero if the distribution is symmetrical. It becomes positive (or negative) if the distribution contains outliers to the right (or left). Kurtosis (K, hereafter) is defined using the fourth central moment. It is a measure of whether the data are heavy-tailed or light-tailed. That is, datasets with high kurtosis tend to have infrequent extreme deviations (or outliers). Data sets with low kurtosis tend to have frequent modestly sized deviations or lack of outliers. The kurtosis becomes 3 for normally distributed random variables. Negative (or positive) deviations of K from 3 indicate narrowing (or widening) of the distribution (e.g. Baillard et al., 2014).

To set up the STA/LTA trigger algorithm, parameters like STA and LTA window durations (in energy channels) and trigger threshold level are crucial. There's no universal rule; settings depend on the application's goal and noise conditions. Practical experience guides optimal trigger settings, typically determined through trial and error. For best results, adjusting parameters gradually is necessary. STA duration should exceed typical peak periods, making triggering sensitive to short events. Longer LTA duration filters out irregular noise fluctuations. Akram and Eaton (2016) offer guidance on parameter selection. Using a larger window approximates the event zone, followed by a smaller window for accurate picking. The trigger threshold level largely determines recorded events, with higher thresholds reducing false triggers. Window length must suit sampling frequency and filtering to avoid biased estimates and ensure accurate peak detection.

2.3. Automatic picking procedure

To identify and characterize spectra which exhibit photoelectron signatures, we have designed and developed an automated method that follows four major steps explained in detail below. We present an automatic picking algorithm for photoelectron detection and characterization and apply it to CAPS-ELS using signal analysis by short term average/long-term average (STA/LTA)- and CF -based detectors. We improve pick precision by computing the CF with higher order statistics. Skewness and kurtosis-derived methods in the datasets are implemented to allow more accurate picking. Once detections are picked, our procedure establishes the pick type using five statistical parameters (a "quintuple") and sets a pick quality index (hearafter QI) based on these and also SNR. These parameters help shape the quality of the photoelectron peak detection. If more parameters are compared simultaneously the detection becomes more reliable.

In this paper, quality is defined as the extent to which a photoelectron peak complies with its signature's standards which are based on the peaks near 24 eV and a decrease in electron intensity above 60 eV due to the drop in the solar spectrum near 20 nm (e.g. Nagy et al., 1977; Gan et al., 1992; Cravens et al., 2009; Galand et al., 2010).

The algorithm classifies detected photoelectrons into one of three quality categories. The QI is a scale designed to help characterize photoelectrons in the spacecraft data. The QI was developed with several goals: 1) to provide a standardized measure of photoelectron peak quality; 2) to discriminate between "the best" and "the least best" ones; 3) to provide an index that is easy for researchers to interpret and 4) to provide a brief, useful assessment of a variety of photoelectron peaks.

The robustness and reliability of the suggested algorithm is tested by comparing manually derived detections, serving as reference picks, with the corresponding automatically estimated detections. Acceptable measures of internal homogeneity, consistency (test-retest reliability) and validity were obtained using statistical hypothesis tests. The utility of the algorithm is illustrated through several examples based on data from all available Titan flybys and also a more detailed look at one specific flyby, the Titan 40 ("T40") flyby. The most important benefits of automated techniques are their consistency and their capability of processing large data sets. The modular design of the algorithm enables the substitution of alternative strategies in any of the four process steps.

To simplify the algorithm's usage, each step has only a few variable parameters. Therefore, in order to optimize the efficiency of the search, the programme is provided with full detection capability and makes use of a high degree of automation, aimed at minimizing the expert's workload. In fact, the modular structure of the program will allow us to develop it with new

and improved capabilities. Future developments in APP will concern the application of other detection algorithms or/and routines to recognize secondary peaks. All photoelectron identification results can be accessed via Caro-Carretero, & García- Jiménez (2023). For more details, see Caro-Carretero et al. (2019) and Cao et al. (2020).

The traditional approach to automatic phase detection has been to apply a series of narrow bandpass frequency filters (that passes frequencies within a certain range -the single count level of ELS- and rejects (attenuates) frequencies outside that range. According to Figure 1 the suggested iterative algorithm can be described as a four-stage process consisting of:

Figure 1.

Flowchart for the four-step algorithm

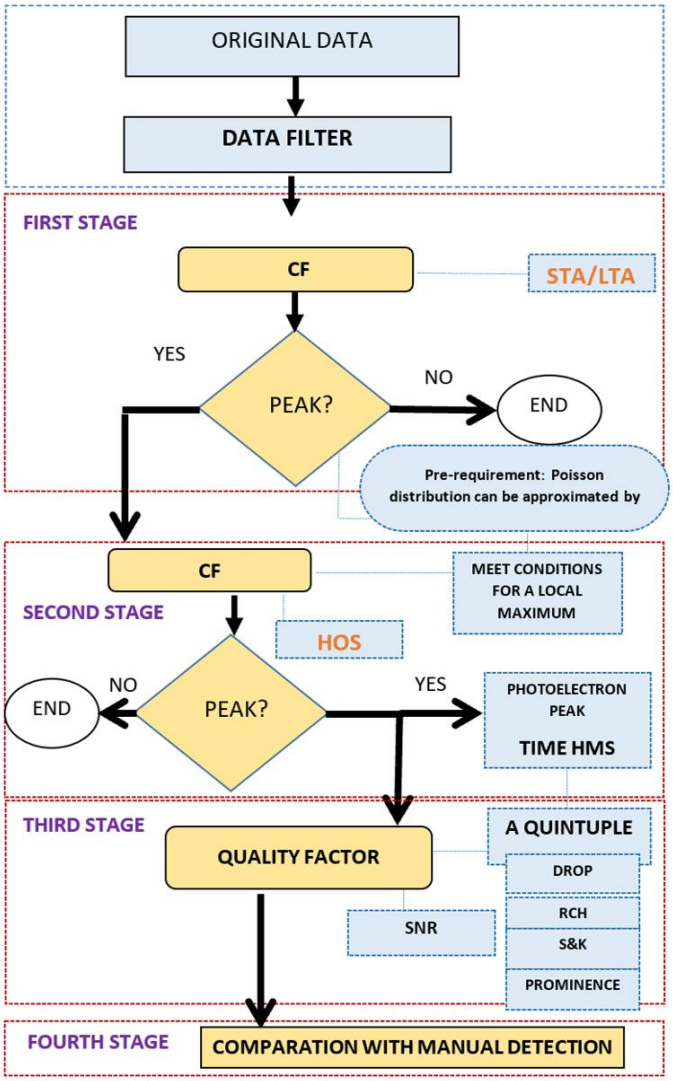

Note: DROP (decrease in electron intensity); RCH (Relative Change of DEF); S (Skewness); K (Kurtosis), P (Prominence)

Source: Own elaboration (2024)

Stage 1
Computation of the CF of a local event using (STA/LTA)-based ratio to individuate the fast variation in the signal by taking the averages over the samples in a time interval of 3 individual 2s raw spectra from start time behaving like a filter.

Stage 2
Calculation of the CF using higher order statistics with a 7-energy channel length long-term window to increase the reliability of photoelectron energy peak detection and time estimation. Considering data was processed using MSSL's Cassini data analysis system. Assuming the data has a Poisson distribution, it can be well approximated by a Gaussian and hence the errors on the spectra are one standard deviation (for details, see Figures 2-4 in T40 flyby). The error bars should cover ±1 standard deviation (68% probability for values of the distribution).

Stage 3
Computation of a quintuple using statistical criteria in order to determine the pick type and estimation of the quality factor using SNR ratio and the quintuple in attempting to differentiate photoelectron peaks and how statistically significant the 24 eV peak is. After the automatic picking algorithm is applied, a complete set of different output parameters is available. The quintuple is composed of 1) the energy where we see the drop in the observed spectrum; 2) relative change (RCH) used as a quantitative indicator of quality assurance between two DEF values, which are the value identified as peak and the value before; relative change is expressed by a ratio as the number of times the DEF value at 24,1 eV is compared with the DEF at the previous energy channel (the more RCH the steeper the slope since the width of the frequency distribution increases with decreasing slope); 3) Skewness as a measure of symmetry; 4) Kurtosis (or excess kurtosis if we consider K minus 3) as a descriptor of the shape of a probability distribution which quantifies the degree of its peakedness; 5) The prominence (P) of the peak to measure how much the peak stands out due to its intrinsic height and its location relative to other peaks. A low isolated peak can be more prominent than one that is higher but is an otherwise unremarkable member of a wide range. Prominence characterizes the height of a peak by the vertical distance between it and the lowest contour line encircling it but containing no higher peak within it. To measure the prominence of a peak we reach the left or right end of the signal on the peak this point being either a valley or one of the signal endpoints. The higher of the two specifies the reference level. The height of the peak above this level is its prominence. We define a ratio between it and its reference level. While the quintuple serves as a local quality estimate, the SNR gives a more global quality estimate of the photoelectron energy peak. We observe the change in the STA/LTA value is not as steep for SNR<2,6 suggesting that it is more challenging to select an optimal detection threshold for relatively lower SNR. As a result, we identified categories 1 and 2 as SNR≤2,6 (Baillard, 2014).

Stage 4
Comparison of manually derived detections. The robustness and reliability of the suggested algorithm is tested by comparing manually derived detections, serving as reference picks, with the corresponding automatically estimated detections from 24 Titan flybys. The thresholds for the quintuple and SNR assigned to the weighting classes 1-3 are summarized in Table 1, where quality factor-1 peaks denote "a clear drop" between 45-70 eV, quality factor-2 peaks are identified by a drop below 45 eV or above 70 eV, and quality factor-3 peaks correspond to all other cases. Scientifically, the presence of this drop in intensity is an additional clear characteristic of primary photoelectron production (Galand et al., 2010). Cases where it is not clearly present can be linked to counting statistics being close to the noise level. Therefore, the QI gives an indication of how clearly the scientific characteristics can be observed in the spectra.

Table 1.

Quality factor scheme for automatic picking

Quality Index	Drop energy	RCH	P	SNR
1	Clear drop present between 45-70 eV (e.g see Figure 2)	1,4≤ RCH ≤2	2≤P≤3	1,6≤SNR ≤2,6
2	Drop present at 30-45 eV or at 70-120eV (e.g. see Figure 3)	1,4≤ RCH ≤2	2≤P≤3	1,8≤SNR≤2,6
3	All other cases, i.e. no clear drop detected (e.g. see Figure 4)	RCH≤1,4	P≤2	SNR≥2,6

Note: Quality index as well as all the parameters are automatically derived by the proposal algorithm (data has been recorded as a comma-delimited ASCII text file, with individual files typically spanning 24 h); RCH (Relative Change); P (Prominence); SNR (Signal-to-Noise Ratio)

Source: Own elaboration

Descriptive statistics and one-way analysis of variance (ANOVA) were used to contrast photoelectron peak features of QI categories. The six parameter scores of the QI had an overall reliability coefficient (Cronbach's α) of 0,92, indicating a high degree of internal consistency. In other words, each of the six parameters appears to measure a particular aspect of the same overall quality constructor. Multiple paired t-hypothesis tests (ANOVA) for the six individual parameter scores showed statistical significant differences between QI categories (p-value<0,1).

The APP then assigns a quality index to photoelectron energy peak obtaining a catalog of picked photoelectron energy times and its features. For each flyby, the APP designed and developed for this algorithm saves all information in a file (Caro-Carretero, & García- Jiménez, 2023).

The picker has a small number of relatively simple user-defined parameters and should be easily adaptable to any dataset. However, we could observe that some limitations of the algorithm performance and picking occur for the case of weak peaks where the pick could be missed entirely since the threshold is generally set too high, and the trigger is made on the following stronger peak.

3. Results

We tested our algorithm on the Cassini data and confirmed the efficiency of the algorithm by comparing the results with manually inspected results from 24 Titan flybys. In order to provide an example of the data set and results that the algorithm can produce, we show data from the Cassini T40 flyby (see Figures 2-4) which was investigated as a photoelectron case study by Wellbrock et al. (2012). The T40 flyby took place on 5 January, 2008 with closest approach at an altitude of 1014 km at 21:30 UT.

Figure 2.

Example of photoelectron quality index 1 (clear drop present between 45-70 eV)

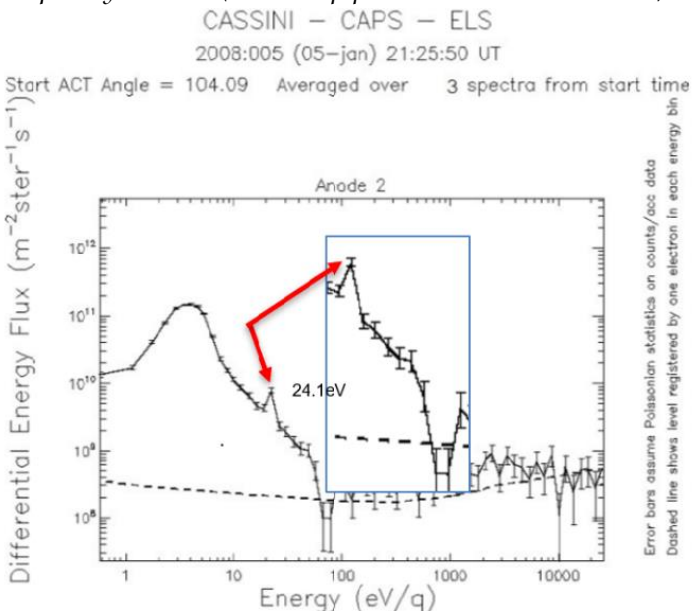

Note: ELS data from the T40 Titan flyby. Six-second averaged (three spectra) differential energy flux (DEF) spectrum starting 21:25:50: UT. The dashed line indicates the single count level of ELS. The arrow in each spectrum points at the 24,1eV photoelectron peak. Error bars assume Poissonian statistics on counts/acc data.

Source: Own elaboration

Figure 3.

Example of photoelectron quality index 2 (drop present at 30-45 eV or at 70-120eV)

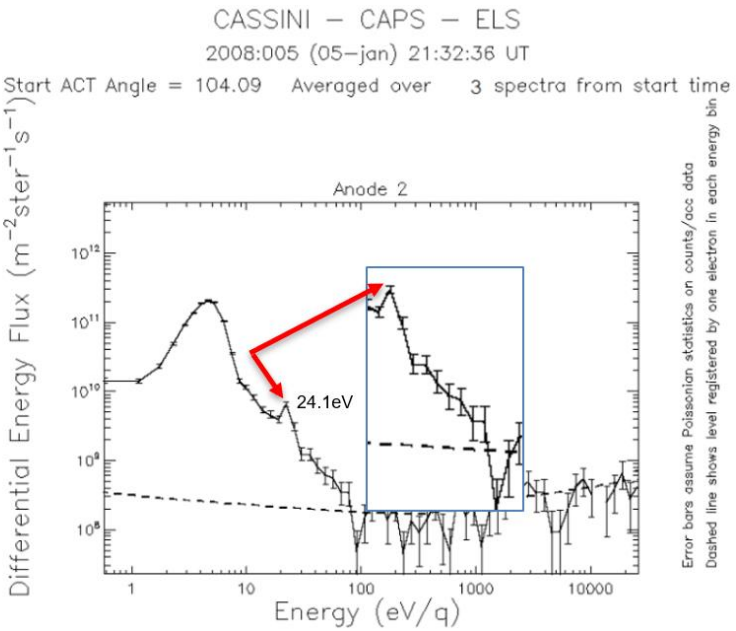

Note: ELS data from the T40 Titan flyby. Six-second averaged (three spectra) differential energy flux (DEF) spectrum starting at 21:32:36: UT. The dashed line indicates the single count level of ELS. The arrow in each spectrum points at the 24,1eV photoelectron peak. Error bars assume Poissonian statistics on counts/acc data.

Source: Own elaboration

Figure 4. 7

Example of photoelectron quality index 3 (no clear drop detected).

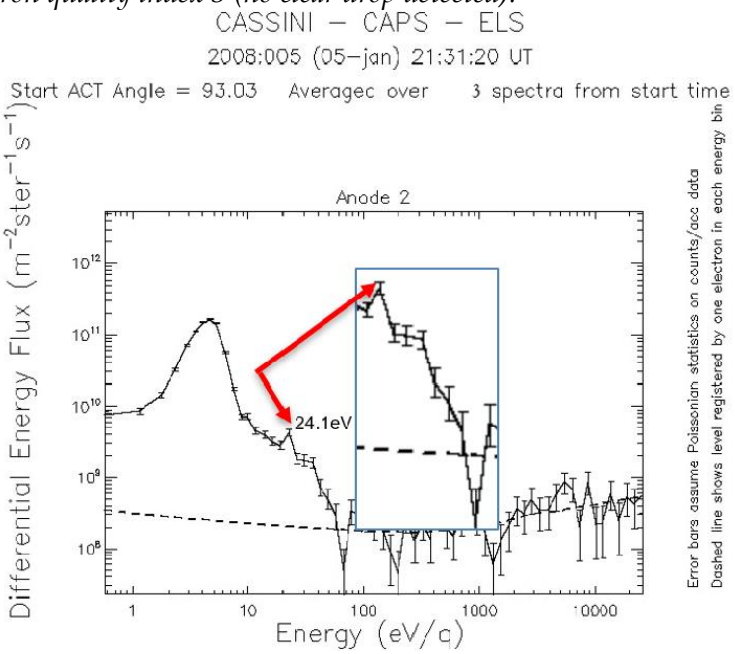

Note: Cassini CAPS-ELS data from the T40 Titan flyby. Six-second averaged (three spectra) differential energy flux (DEF) spectrum starting at 21:31:20: UT. The dashed line indicates the single count level of ELS. The arrow in each spectrum points at the 24,1eV photoelectron peak. Error bars assume Poissonian statistics on counts/acc data.

Source: Own elaboration

There is evidence for magnetic connections to local production sites far from Titan during this flyby. During this flyby 206 peaks were detected and classified according to the quality index as presented in Table 2.

Table 2.

The assigned pick quality index for T40 Flyby

Quality Index	Number of peaks
1	11
2	18
3	177
Total	**206**

Source: Own elaboration

Our automatic picking algorithm can also be applied to larger data sets such as the complete set of electron data from all Titan 62 flybys where CAPS was operating. This will allow studying the spatial distribution of photoelectron peaks near Titan. We provide here a general example of the data set provided by the algorithm. A more detailed scientific analysis using the algorithm to study Titan's magnetic environment has been the focus of recent studies, e.g. Cao et al. (2020).

4. Discussion

Figure 5 shows an overview of all photoelectron peaks detected as a result of applying the algorithm to CAPS-ELS data from the 62 Cassini Titan flybys. In 56 of them the 24,1 eV photoelectrons were detected. Every black dot indicates an observation of a photoelectron peak. The distance is measured from Titan's surface in Titan radii (one Titan radius, RT, is about .2574 km). Solar zenith angle (SZA) is measured from the subsolar point; a SZA beyond the terminator (90º) is considered to be the nightside, even though we should note that at these high altitudes solar radiation can still reach parts of the atmosphere beyond the terminator.

Figure 5.

Spatial distribution of photoelectron peak observations near Titan found by the algorithm when applied to CAPS-ELS data from 62 Cassini Titan encounters.

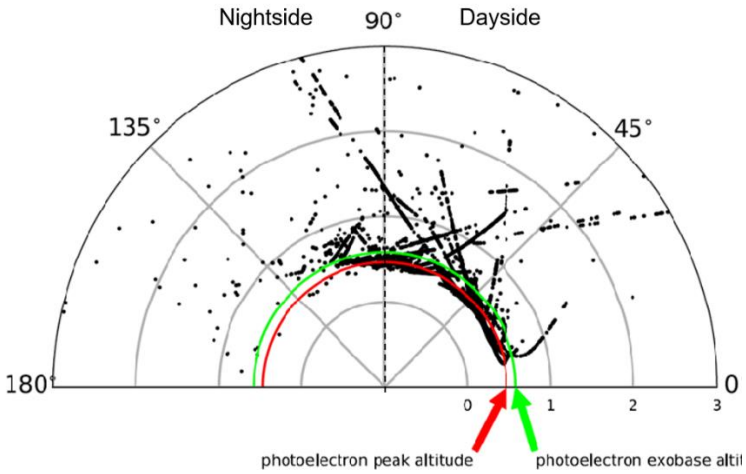

Note: The radial distance from the center shows the distance from Titan in Titan radii (RT = 2.574 km). The angles shown are SZA (Solar Zenith Angle). The photoelectron peak altitude (~1.200 km) and the photoelectron exobase altitude (~1.500 km) are shown as red and green lines, respectively.

Source: Own elaboration

The results demonstrate that 35% of the photoelectron peak observations are found outside the dayside ionosphere, indicating that there are magnetic field lines connecting the day and night side and allowing photoelectrons to travel along these to the observation sites on the nightside. As the SZA increases from 90º to 180º, the number of photoelectron peak observations decreases, demonstrating that the deep night side is less well connected to the lower dayside ionosphere, where solar fluxes generate most of photoelectrons. These aspects have been explored further in recent studies such as Cao et al. (2020).

In Figure 6 we show what the plot shown in Figure 5 looks like for one specific Titan flyby and again use T40 as an example. The colours specify which instrument anode was used; the anodes point in different directions and can therefore provide information about the electron distributions. The position of anode N has been shifted sideways by (N-2)*0,1 RT to distinguish it clearly from the neighbouring anodes. Figure 6 reveals that in the dayside ionosphere, at an altitude near 0,5 RT and SZA less than 90 o, all anodes observed continuous photoelectron peaks. This is a strong indication for a locally produced photoelectron population because the distribution appears to be more isotropic (i.e. observed in any direction). The observations at higher altitudes on the other hand are seen in specific anodes only; their distributions are therefore less isotropic, indicating that they are likely to have travelled to the observation sites via magnetic field lines (i.e. very directional motion). This agrees with the theory that

photoelectrons are produced in the lower dayside ionosphere where neutral particles can be ionized by solar radiation, and then travelled from there to higher altitudes and/or the nightside, as shown by Wellbrock et al. (2012) in this T40 case. Local production at higher altitudes is less likely due to lower neutral densities. Investigating the distributions of photoelectrons can be enhanced by studying their pitch angle distributions (i.e. how close the direction of motion is compared to the magnetic field direction), which will also be a focus of future studies such as Cao et al. (2020) to study Titan's plasma environment in more detail using the algorithm described in this study. The example results presented in Figure 6 also agree well with the photoelectron peaks found by Wellbrock et al. (2012), who manually inspected the T40 electron spectra to locate the peaks.

Figure 6.

Spatial distribution of photoelectron peak observations near Titan found by the algorithm when applied to CAPS-ELS data from one specific Titan flyby: T40.

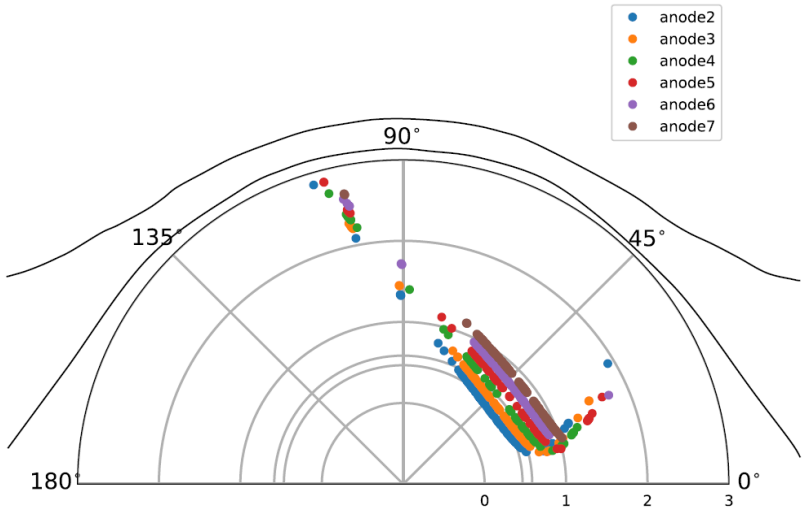

*Note: The radial distance from the centre shows the distance from Titan in Titan radii (RT = 2574 km), and the angles show the SZA (Solar Zenith Angle). The position of anode N has been shifted sideways by (N-2)*0,1 RT to distinguish it clearly from the neighbouring anodes. The grids below 1 RT indicates the photoelectron peak altitude and the photoelectron exobase altitude, respectively. Saturn's nominal magnetospheric plasma flow comes from the top during this flyby.*

Source: Own elaboration

5. Conclusions

We have designed and developed a new automated four-step method to determine the locations of 24eV photoelectron peaks in Titan's plasma environment and characterized these using a quality factor. It has been applied to data from all Titan flybys using signal analysis. The algorithm can be a powerful tool to automatically detect photoelectron energy peaks with high accuracy and precision and coherently assigning their quality index.

Advancements in our understanding of planetary plasma environments through photoelectron peak detection can lead to the development of sustainable space exploration technologies. By studying spatial distributions of photoelectron peaks, scientists can design more efficient spacecraft propulsion systems, leading to reduced resource consumption and environmental impact in space exploration endeavors. Understanding planetary plasma environments is crucial for predicting and mitigating the impacts of space weather events on Earth's climate. By studying photoelectron peaks, scientists can improve models that forecast space weather phenomena, allowing for better preparation and mitigation strategies to safeguard critical infrastructure, such as satellite networks and power grids, thereby contributing to climate resilience. Photoelectron peak detection contributes to our

understanding of the composition and dynamics of celestial bodies like Titan. This knowledge informs sustainable resource management practices for future space missions, ensuring the responsible extraction and utilization of resources while minimizing environmental impact.

Additionally, understanding planetary environments supports planetary protection efforts, preserving celestial bodies and their potential for scientific exploration. Furthermore, research on planetary plasma environments and photoelectron peak detection fosters public awareness and engagement in space exploration and environmental stewardship. By communicating the importance of studying celestial bodies and their atmospheres, including the role of photoelectron peaks, scientists can inspire future generations to pursue careers in science, technology, engineering and mathematics (STEM) fields, driving innovation and sustainable development efforts. In conclusion, the study of photoelectron peaks and planetary plasma environments contributes to sustainable development by informing the development of sustainable space technologies, supporting climate change mitigation efforts, promoting responsible resource management practices, and fostering public engagement in science and environmental stewardship. Then, photoelectron peak detection and the study of planetary plasma environments contribute to SDG 9 (Industry, Innovation, and Infrastructure) by fostering innovation and technological advancement in the field of space exploration.

By enhancing our understanding of planetary systems, we can develop more efficient and sustainable technologies for space exploration and colonization. This includes the development of cleaner and more efficient propulsion systems, as well as the creation of space infrastructures that minimize environmental impact. While knowledge of photoelectron peaks on Titan would not provide direct solutions to mitigating climate change on Earth, it could have significant implications for improving our understanding of climate overall and for developing technologies and strategies to address climate challenges on our own planet.

6. References

Aguirre, C., Franzese, G., Esposito, F., Vázquez, L., Caro-Carretero, R., Vilela-Mendes, R., Ramírez-Nicolás, M., Cozzolino, F., & Popab, C.I. (2017). Signal-adapted tomography as a tool for dust devil detection. *Aeolian Research*, 29, 13-22. https://doi.org/10.1016/j.aeolia.2017.09.005

Akram, J., & Eaton, D.W. (2016). A review and appraisal of arrival-time picking methods for downhole microseismic data. *Geophysics*, *81* (2), KS71-KS91. https://doi.org/10.1190/geo2014-0500.1

Allen, R. (1982). Automatic phase pickers: Their present use and future prospects. *The Bulletin Of The Seismological Society Of America*, *72*(6B), S225-S242. https://doi.org/10.1785/bssa07206b0225

Baillard, C., Crawford, W. C., Ballu, V., Hibert, C., & Mangeney, A. (2014). An automatic Kurtosis-based P and S phase picker designed for local and regional seismic networks. *The Bulletin Of The Seismological Society Of America*, 104, 394-409. https://doi.org/10.1785/0120120347

Brown, R.H., Lebreton, J-P, & Waite, J.H. (Eds) (2010). *Titan from Cassini-Huygens*. Springer Science+Business Media B.V. https://doi.org/10.1007/978-1-4020-9215-2

Cao, Y.-T., Wellbrock, A., Coates, A. J., Caro-Carretero, R., Jones, G. H, Cui, J., Galand, M., & Dougherty, M. K. (2020). Field-aligned photoelectron energy peaks at high altitude and

nightside of Titan. *Journal of Geophysical Research: Planets*, *125*(1) https://doi.org/10.1029/2019JE006252

Caro-Carretero, R., Wellbrock, A., & Cao, Y. (2019). *Cassini ELS Photoelectron identification*. Mendeley Data. http://dx.doi.org/10.17632/dwxhzbnvr9.1

Caro-Carretero, R. & García-Jiménez, F. (2023). Impact of the implementation of the new quarter-hourly model on a wind farm in the peninsular electricity system. *DYNA*, 98, 486-580. https://doi.org/10.6036/10882

Coates, A. J., Johnstone, A. D., Sojka, J. J., & Wrenn, G. L. (1985). Ionospheric photoelectrons observed in the magnetosphere at distances up to 7 Earth radii. *Planetary and Space Science*, 33, 1267-1275. https://doi.org/10.1016/0032-0633(85)90005-4

Coates, A. J., McAndrews, H. J., Rymer, A. M., Young, D. T., Crary, F. J., Maurice, S., Johnson, R. E., Baragiola, R. A., Tokar, R. L., Sittler, E. C., & Lewis, G. R. (2005). Plasma electrons above Saturn's main rings: CAPS observations. *Geophysical Research Letters*, 32, L14S09. https://doi.org/10.1029/2005GL022694

Coates, A. J., Crary, F. J., Young, D. T., Szego, K., Arridge, C. S., Bebesi, Z., Sittler, E. C. Jr., Hartle, R. E, & Hill, T. W. (2007). Ionospheric electrons in Titan's tail: Plasma structure during the Cassini T9 encounter. *Geophysical Research Letters*, 34, L24S05. https://doi.org/10.1029/2007GL030919

Coates, A. J., Jones, G. H., Lewis, G. R., Wellbrock, A., Young, D. T., Crary, F. J., Johnson, R.E., Cassidy, T.A., & Hill, T. W. (2010). Negative ions in the Enceladus plume. *Icarus*, 206, 618-622. https://doi.org/10.1016/j.icarus.2009.07.013

Coates, A. J., Tsang, S. M. E., Wellbrock, A., Frahm, R. A., Winningham, J. D., Barabash, S., Lundin, R., Young, D.T., F.J., & Crary, F. J. (2011). Ionospheric photoelectrons: Comparing Venus, Earth, Mars and Titan. *Planetary and Space Science*, 59, 1019-1027. https://doi.org/10.1016/j.pss.2010.07.016

Coates, A. J., Wellbrock, A., Jones, G. H., Waite, J. H., Schippers, P., Thomsen, M. F., Arridge, C. S., & Tokar, R. L. (2013). Photoelectrons in the Enceladus plume. *Journal of Geophysical Research: Space Physics*, 118, 5099-5108. https://doi.org/10.1002/jgra.50495

Cravens, T. E., et al. (2009). Model-data comparisons for Titan's nightside ionosphere. *Icarus*, 199, 174-188. https://doi:10.1016/j.icarus.2008.09.005

Crósta, Á. P., Silber, E. A., Lopes, R. M. C., Johnson, B. C., Bjonnes, E., Malaska, M. J., Vance, S., Sotin, C., Solomonidou, A., & Soderblom, J. M. (2021). Modeling the formation of Menrva impact crater on Titan: Implications for habitability. *Icarus*, 370, 114679. https://doi.org/10.1016/j.icarus.2021.114679

Dunn, W., Branduardi-Raymont, G., Ray, L., Jackman, C., Kraft, R., Elsner, R., Rae, I.J., Yao, Z., Vogt, M. F., Jones, G. H., Gladstone, G. R., Orton, G. S., Sinclair, J. A., Ford, P. G., Graham, G. A., Caro-Carretero, R., & Coates, A. (2017). The Independent Pulsations of Jupiter's Northern and Southern X-ray Auroras. *Nature Astronomy*, 1, 758–764. http://dx.doi.org/10.1038/s41550-017-0262-6

Fox, J. L., & Dalgarno, A. (1979), Ionization, luminosity, and heating of the upper atmosphere

of Mars. *Journal of Geophysical Research*, 84, 7315-7333. https://doi:10.1029/JA084iA12p07315

Frahm, R. A., Winningham, J. D., Sharber, J. R., Scherrer, J. R., Jeffers, S. J., Coates, A. J., Linder, D.R., Kataria, D.O., Lundin, R., Barabash, S., Holmström, M., Andersson, H., Yamauchi, M., Grigoriev, A., Kallio, E., Säles, T., Riihelä, P., Schmidt, W., Koskinen, H., …, & Dierker, C. (2006). Carbon dioxide photoelectron energy peaks at Mars. *Icarus*, 182, 371–382. https://doi.org/10.1016/j.icarus.2006.01.014

Friedson, A. J., West, R. A., Wilson, E., Oyafuso, F., & Orton, G. S. (2009). A global climate model of Titan's atmosphere and surface. *Planetary And Space Science*, *57*(14-15), 1931-1949. https://doi.org/10.1016/j.pss.2009.05.006

Galand, M., Yelle, R.V., Cui, R. V., Wahlund, J.-E., Vuitton, V., Wellbrock, A., & Coates, A (2010). Ionization sources in Titan's deep ionosphere. *Journal of Geophysical Research*, 115, A07312, https://doi:10.1029/2009JA015100

Gan, L., Keller, C.N., & Cravens, T.E. (1992). Electrons in the ionosphere of Titan. *Journal of Geophysical Research*, *97*(A8), 12137-12151. https://doi.org/10.1029/92JA00300

Gu, H., Cui, J., Lavvas, P., Niu, D., Wu, X., Guo, J., He, F., & Wei, Y. (2019). Dayside nitrogen and carbon escape on Titan: the role of exothermic chemistry. *Astronomy & Astrophysics*, 633, A8. https://doi.org/10.1051/0004-6361/201936826

Haider, S.A. (1986). Some molecular nitrogen emission from Titan-solar EUV interaction. *Journal of Geophysical Research*, 91, 8998-9000. https://doi.org/10.1029/JA091iA08p08998

Hörst, S. M. (2017). Titan's atmosphere and climate. *Journal Of Geophysical Research. Planets*, *122*(3), 432-482. https://doi.org/10.1002/2016je005240

Jackson, B., & Lorenz, R. (2015). A multiyear dust devil vortex survey using an automated search of pressure time series. *Journal Of Geophysical Research. Planets*, 120, 401-412. https://doi: 10.1002/2014JE004712

Linder, D. R., Coates, A. J., Woodliffe, R. D., Alsop, C., Johnstone, A. D., Grande, M., Preece, A., Narheim, B., & Young, D. T. (1998). The Cassini CAPS electron spectrometer. In R. F. Pfaff, J. E. Borovsky, & D. T. Young (Eds.). *American geophysical union geophysical monograph series* (Vol. 102, pp. 257). Washington, DC: American Geophysical Union.

Lorenz R.D, & Lanagan P.D. (2014). A barometric survey of dust devil vortices on a desert playa. *Boundary Layer Meteorology*, 53, 555-68. http://dx.doi.org/101029/2003JE002161

Mitchell, J. L., & Lora, J. M. (2016). The Climate of Titan. *Annual Review Of Earth And Planetary Sciences*, *44*(1), 353-380. https://doi.org/10.1146/annurev-earth-060115-012428

Mulholland, P., & Wilde, S. P. R. (2020). An Iterative Mathematical Climate Model of the Atmosphere of Titan. *Journal Of Water Resource And Ocean Science*, *9*(1), 15. https://doi.org/10.11648/j.wros.20200901.13

Murphy, J., & Nelli, S. (2002). Mars Pathfinder convective vortices: frequency of occurrence. *Geophysical Research Letters*, 29, 2103. https://doi.org/10.1029/2002GL015214

Nagy, A. F., Doering, J. P., Peterson, W. K., Torr, M. R., & Banks, P. M. (1977). Comparison between calculated and measured photoelectron fluxes from Atmosphere Explorer C and E. *Journal of Geophysical Research*, 82, 5099-5103. https://doi.org/10.1029/JA082i032p05099

NASA Space Science Data Coordinated Archive (2023). Accessed 31 May 2024 at https://nssdc.gsfc.nasa.gov/nmc/dataset/display.action?id=PSFP-00374. Data are available on-line from the Planetary Data System (PDS) at: https://pds-ppi.igpp.ucla.edu/data/CO-E_J_S_SW-CAPS-2-UNCALIBRATED-V1.0/

Neubauer, F.M., Gurnett, D. A., Scudder, J. D., & Hartle, R.E. (1984). *Titan's magnetospheric interaction, in Saturn*. University of Arizona. Press.

Ozak, N., Cravens, T. E., Jones, G. H., Coates, A. J., & Robertson, I. P. (2012). Modeling of electron fluxes in the Enceladus plume. *Journal of Geophysical Research*, 117, A06220. https://doi.org/10.1029/2011JA017497

Ringrose T.J., Patel M.R., Towner M.C., Balme M, Metzger S.M., & Zarnecki J.C. (2007). The meteorological signatures of dust devils on Mars. *Planet Space Sci.*, 55, 2151-63. https://doi.org/10.1016/j.pss.2007.07.002

Schippers, P., Blanc, M., André, N., Dandouras, I., Lewis, G. R., Gilbert, L. K., … Dougherty, M. K. (2008). Multi-instrument analysis of electron populations in Saturn's magnetosphere. *Journal of Geophysical Research*, 113, A07208. https://doi.org/10.1029/2008JA013098

Schippers, P., André, N., Johnson, R. E., Blanc, M., Dandouras, I., Coates, A. J., Krimigis, S. M., & Young, D. T. (2009). Identification of photoelectron energy peaks in Saturn's inner neutral torus. *Journal of Geophysical Research*, 114, A12212. https://doi.org/10.1029/2009JA014368

Sylvestre, M., Teanby, N. A., D'Ollone, J. V., Vinatier, S., Bézard, B., Lebonnois, S., & Irwin, P. G. J. (2020). Seasonal evolution of temperatures in Titan's lower stratosphere. *Icarus*, 344, 113188. https://doi.org/10.1016/j.icarus.2019.02.003

Taylor, S. A., Coates, A. J., Jones, G. H., Wellbrock, A., Fazakerley, A. N., Desai, R. T, Caro-Carretero, R., Michiko, M. W., Schippers, P. & Waite, J. H. (2018). Modeling, analysis, and interpretation of photoelectron energy spectra at Enceladus observed by Cassini. *Journal of Geophysical Research: Space Physics*, *123* (1), 287-296. https://doi.org/10.1002/2017JA024536

Tsang, S.M.E., Coates, A. J., Jones, G. H., Frahm, R.A., Winningham, J.D., Barabash, S., Lundin, R., & Fedorove, A. (2015). Ionospheric photoelectrons at Venus: Case studies and first observation in the tail. *Planetary and Space Science*, *113-114*, 384-394. https://doi.org/10.1016/j.pss.2015.01.019

Wellbrock, A., Coates, A. J., Sillanpää, I., Jones, G. H., Arridge, C. S., Lewis, G. R., Young, D.T., Crary, F. J., & Aylward, A. D. (2012). Cassini observations of ionospheric photoelectrons at large distances from Titan: Implications for Titan's exospheric

environment and magnetic tail. *Journal of Geophysical Research*, 117, A03216. https://doi:10.1029/2011JA017113

Xiong, S., Muller, J., & Caro-Carretero, R. (2018). A New Method for Automatically Tracing Englacial Layers from MCoRDS Data in NW Greenland. *Remote Sensing*, *10*(1), 43. https://doi.org/10.3390/rs10010043 and http://www.mdpi.com/2072-4292/10/1/43

Young, D. T., Berthelier, J. J., Blanc, M., Burch, J. L., Coates, A. J., Goldstein, R., Grande, M., Hill, T. W., Johnson, R. E., Kelha, V., Mccomas, D. J., Sittler, E. C., Svenes, K. R., Szegö, K., Tanskanen, P., Ahola, K., Anderson, D., Bakshi, S., Baragiola, R. A., …, & Zinsmeyer, C. (2004). Cassini plasma spectrometer investigation. *Space Science Reviews*, 114, 1–112. https://doi.org/10.1007/s11214-004-1406-4

CONTRIBUCIONES DE AUTORES/AS, FINANCIACIÓN Y AGRADECIMIENTOS

Funding: This research did not receive any external funding.

Acknowledgements: I sincerely thank D. Fernando García Jiménez for their valuable collaboration and support in the development of this work. Their expertise and dedication have been instrumental to the success of this research.

AUTOR:

Raquel Caro-Carretero
Universidad Pontificia Comillas de Madrid. Cátedra de Catástrofes Fundación AON España. España.

La Dra. Raquel Caro-Carretero, como Profesora Propia Adjunta en el Departamento de Organización Industrial de la Escuela Técnica Superior de Ingeniería (ICAI) de la Universidad Pontificia Comillas de Madrid, cuenta con una amplia experiencia docente como investigadora. Su trabajo abarca diversas áreas, desde la aplicación de la estadística en campos ingenieriles y económico-financieros hasta el análisis de migraciones, turismo, catástrofes y Ciencias del Espacio. Es responsable de la Cátedra de Catástrofes Fundación AON España en Comillas. Durante una década, también ha compartido su conocimiento en la Facultad de Ciencias Económicas y Empresariales de Comillas (ICADE). Su compromiso con la excelencia académica y su dedicación a la investigación se reflejan en su participación activa en conferencias internacionales, colaboraciones interdisciplinarias y publicaciones en revistas de alto impacto.
rcaro@comillas.edu

Índice H: 9
Orcid ID: 0000-0003-2233-7635
Scopus ID: 56069981700
Google Scholar: https://scholar.google.es/citations?user=w-erjeoAAAAJ&hl=es
ResearchGate: https://www.researchgate.net/profile/Raquel-Caro-Carretero